COO-4759-2

CONF-790811 2--1

RATE MEASUREMENT IN SHOCK WAVES WITH THE LASER-SCHLIEREN TECHNIQUE

J.H. Kiefer and J.C. Hajduk

Department of Energy Engineering

University of Illinois at Chicago Circle, Chicago, Illinois 60680 USA

We discuss the laser-schlieren or narrow laser beam deflection technique in some detail, with particular reference to its application to very fast processes. The technique is first briefly reviewed together with selected previous applications. The optics of the beam-shock wave interaction is then examined using the scalar formulation of Huygens' principle (Kirchoff integral), with the shock density profile introduced as a transmission coefficient. The accuracy with which the signal generated by a differential detector will reproduce the variation of the refractive index gradient in a reactive shock is discussed in terms of this formulation. The response of such a detector to passage of a curved shock in a rare gas is also determined employing the shock-curvature theory of de Boer. These calculations are in good agreement with experiment and locate the "time origin" - coincidence of shock leading edge and beam center - on the "positive" portion of the signal near zero-crossing; an assignment which is in disagreement with the earlier calculations of Dove and Teitelbaum. This time origin shift and the averaging of initiation over a curved front can combine to generate a large correction of total density change measurements in relaxation experiments.

INTRODUCTION

Since its introduction in 1965(1), the laser-schlieren, or narrow laser beam deflection technique, has been used in the study of a broad range of kinetic phenomena in shock waves (2). Its virtues of simplicity, direct recording of rate, and excellent temporal/spatial resolution make it particularly suited to the observation of fast processes. It has accordingly been extensively employed in the study of relaxation in diatomics and polyatomics, the dissociation of diatomics, and the decomposition of a growing number of polyatomic species.

When the method is "pushed", as in the resolution of extremely rapid processes such as relaxation in H_2 (3) (4) (5), relaxation of many polyatomics (2), and the measurement of dissociation induction times (6), a very detailed analysis of the schlieren signal becomes imperative. The "time origin" must now be very accurately located; and since the characteristic length ($u\tau$) for such processes can become comparable to the axial extent of the curved shock

DISCLAIMER

z_c, the axial "spread" of initiation over the curved front must also be taken into account.

Here we consider the above problems in some detail. In particular we present a rather rigorous treatment of the optics of the beam-shock interaction using the scalar formulation of Huygens' principle (Kirchoff integral) (7) (8). With this we are able to reproduce the signals generated by a rare-gas shock quite accurately. The analysis permits a decisive location of the coincidence of shock leading-edge and beam center, which is a starting point for the consideration of process initiation. We begin with a brief review of the technique.

I.) THE LASER-SCHLIEREN TECHNIQUE

A schematic of a typical modern set-up is shown in Fig. 1. The parallel beam from a He-Ne laser (6328Å) traverses the shock tube normal to the flow, and after some distance is intercepted by a differential detector (photodiode). Angular deflection of the beam produces a differential voltage which is recorded. The angular sensitivity may be calibrated by rotating the indicated mirror at a known speed. For small deflections the voltage-angular deflection relation is linear (23).

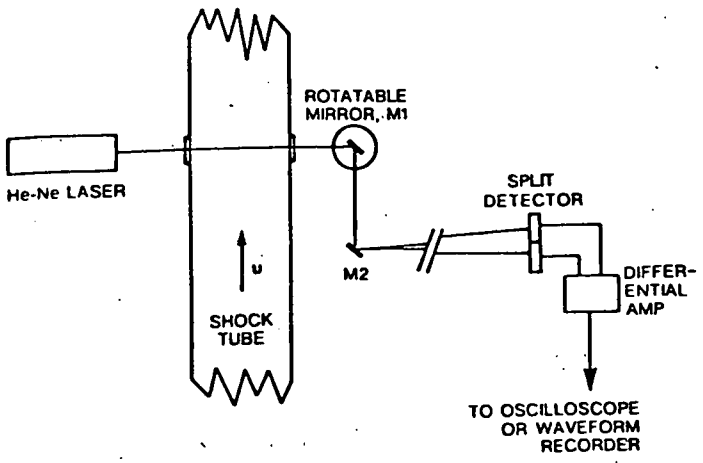

Fig. 1. Schematic of a "typical" modern laser-schlieren apparatus

The incident beam has the familiar Gaussian power distribution (7)

$$P(x,y) = P_o \left(\frac{2}{\pi a^2}\right) \exp - \left(\frac{2(x^2 + y^2)}{a^2}\right) \qquad [1]$$

Where P_o is the total beam power, and a_o is the e^{-2} radius. Typical values are $0.2 < a_o < 0.65$ mm and P_o = 1-8 mw. As the beam traverses the system it retains its Gaussian form, but diffraction increases the radius. At distance D, the radius has grown to

$$a = a_o \left(1 + \left(\frac{\lambda D}{\pi a_o^2}\right)^2\right)^{1/2} \qquad [2]$$

The detector distance is usually large (3-10m) so the radius at the detector is 2-20 a_o.

When higher derivatives of the refractive index may be neglected (see below), the beam is simply deflected through an angle

$$\Theta = \int_{-W/2}^{W/2} \frac{dn}{dx}\, d\omega \qquad [3]$$

where W is the shock tube diameter and dn/dx the refractive index gradient along the tube axis. With a constant gradient across the tube as in a reactive but ideal plane shock, $\Theta = W(dn/dx)$; and if the gas refractivity is constant, the angular deflection is proportional to the density gradient $\Theta = KW\,(d\rho/dx)$. This gradient is directly proportional to the net rate of endothermic reaction in an ideal shock (2) (10), and the resulting proportionality of recorded signal and rate of reaction is a unique feature of the technique.

The narrow beam affords a high spatial resolution (0.1 mm is typical), and the large signal-to-noise ratio possible with modern detectors allows a commensurate speed of response while retaining a very high sensitivity to deflection. The useful resolution and sensitivity are usually limited only by shock nonideality, i.e., front curvature and early boundary layer.

II.) EXPERIMENTS

The advantages of the technique as well as its limitations are most easily delineated by consideration of a few selected experiments. Direct recording of rate and high spatial/temporal resolution allow the determination of "initial" rates for many reactions. There are some difficulties with the specification of an unambiguous initial rate for decomposition reactions (10) (11), but this does not appear too serious a problem in most cases. The usual advantages of initial rate determination - known composition and state, simpler mechanism - together with the improvement in precision which can result from direct rate measurement are nicely illustrated by the work of Breshears, Bird, and Kiefer (10) on O_2 dissociation. Their data for the dissociation rate coefficient in krypton diluent are shown in Fig. 2.

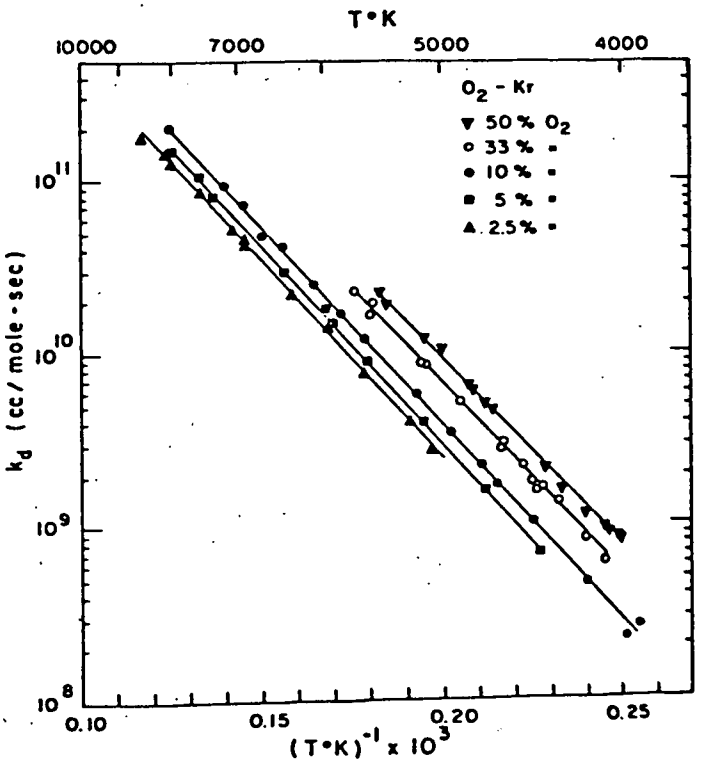

Fig. 2. Values of the effective dissociation rate coefficient k_d $[d(O_2)/dt = -k_d(O_2)(M)]$ obtained for mixtures of O_2 in Kr (10). The solid lines are independent least-squares fits of the Arrhenius expression, $k_d = A \exp(-E/RT)$, to the data for each mixture composition.

The technique is also useful in the extraction of primary dissociation rates in heteronuclear decomposition where fast secondary reactions often interfere. To illustrate we consider the decomposition of HCl as studied by Breshears and Bird (12). The mechanism is presumably

$$HCl + M \rightarrow H + Cl + M \quad \{1\}$$

$$H + HCl \rightarrow H_2 + Cl \quad \{2\}$$

$$Cl + HCl \rightarrow Cl_2 + H \quad \{3\}$$

$$H_2 + M \rightarrow 2H + M \quad \{4\}$$

$$Cl_2 + M \rightarrow 2Cl + M \quad \{5\}$$

If the rate is caught very early, only reactions {1} and {2} should be significant. But reaction {2} is nearly thermoneutral (~1kcal exothermic) whereas the dissociation is 102.2 kcal endothermic. Since the schlieren signal is proportional to the net rate of endothermic reaction, reaction{2} has negligible effect regardless of its rate. This feature of fast but nearly thermoneutral secondary reaction is not uncommon in polyatomics and has been exploited in CH_4 (13) (14), CO_2 (15), SO_2 (16), and C_2H_6 (17).

The relaxation of H_2 (3) (4) (5) (18) (19) is perhaps the prime example of an extremely rapid process which requires maximum sensitivity and resolution. The very small relaxing heat capacity, low refractivity, and low molecular weight - which necessitates dilution with a heavy rare gas - prohibit slowing the relaxation with reduced pressure, as only when the process is very rapid is the gradient large enough to be discernable. An example oscillogram showing H_2 relaxation is given in Fig. 3, and a semilog plot of this signal is shown in Fig. 4. The slope of the latter provides the relaxation time. If the line is extrapolated to t = 0, giving an "initial" gradient ρ_i', the net density change for the process is $\Delta\rho_o = u\tau\rho_i'$. Here τ is the (laboratory) relaxation time. The expected $\Delta\rho_v$ for pure vibrational relaxation is easily calculated and the ratio $\Delta\rho_o/\Delta\rho_v$ determined. In nearly every case this ratio is found to exceed unity (4) (18). In fact, Dove and Teitelbaum (4) obtained some ratios as large as 4. There is obviously a serious difficulty here which led these authors to suggest a strong rotational involvement in the relaxation (19) (4).

Of all the kinetic studies using the laser-schlieren technique, the work of Dove, Nip, and Teitelbaum (6) on N_2O pyrolysis most impressively illustrates its possibilities. From an extensive series of experiments covering the range 450 - 3590 K, these authors derived relaxation times, rates of primary dissociation, summed rates of two secondary reactions, and induction times for the primary dissociation. The measurements of induction time are unique; no such measurement has ever been reported for any other polyatomic species.

The major features of the N_2O pyrolysis mechanism were considered well-known by Dove et. al., although they ultimately did find indirect evidence suggesting one or more additional reactions may be occuring. The mechanism they employed is

$$N_2O + M \rightarrow N_2 + O + M \quad (\Delta H \sim + 38 \text{ kcal/mole}) \quad \{1\}$$

$$O + N_2O \rightarrow N_2 + O_2 \quad (\Delta H \sim - 79) \quad \{2\}$$

$$O + N_2O \rightarrow 2\,NO \quad (\Delta H \sim -36) \qquad \{3\}$$

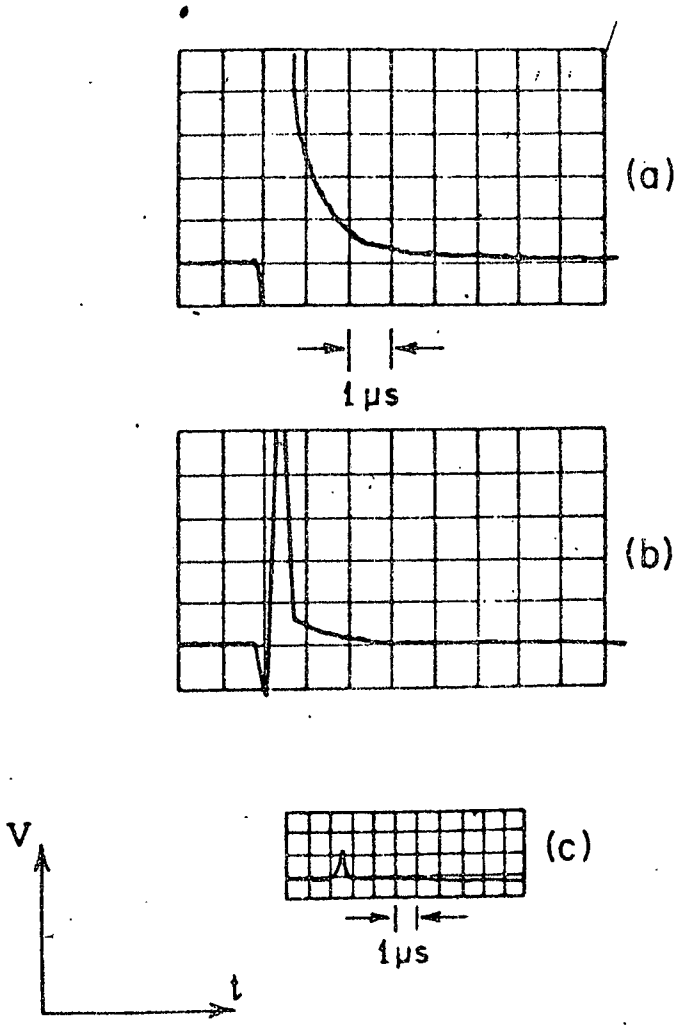

Fig. 3. Schlieren oscillogram tracings showing vibrational relaxation in a 30% H_2 - 70% Ar mixture (5). Horizontal axis is laboratory time and vertical axis is detector output voltage in each case. u = 1.989 mm/μsec, P_o = 9.1 Torr, a_o = 0.58 mm, D = 2m, and W = 7.62 cm. (a) Measure of axial density gradient showing exponentially decaying relaxation signal. $\Delta V/V_o P_o$ = 0.0231 per major division. (b) Less-amplified version of signal in (a) showing modulation due to shock front as well as the relaxation signal. $\Delta V/V_o P_o$ = 0.1153 per major division. (c) Measure of total laser power incident on photodiode as a function of time. The spike indicates that a significant portion of the light is deflected off the detector during passage of the shock front. $\Delta V/V_o P_o$ = 0.1774 per major division. (Courtesy J.E. Dove).

Example oscillograms showing pyrolysis are given in Fig. 5, where the temperature increases in the order of presentation. The first record (a), at 1950 K, shows relaxation followed by a very weak and slowly decaying dissociation gradient. Oscillogram (b) shows a (poorly resolved) relaxation followed by endothermic reaction (positive gradient), which finally tails into a weak exothermicity (negative gradient). In (c), relaxation is lost in the shock-front signal and the endothermic dissociation is quickly overwhelmed by a strong exothermicity. Finally, in (d) even the endothermic reaction {1} is nearly lost and, effectively, only the exothermic region appears. The complexity of such records should permit extraction of more than just the rate of {1}, and, recognizing this, Dove et. al. analyzed the entire gradient profile using both an approximate analytic solution of the kinetic equations for the above mechanism and a direct computer simulation. Consequently, they determined not only the rate of {1} but also the sum of the rates of {2} and {3}. The vibrational relaxation zone being of finite length, even though often unresolved, the onset of reaction is presumably delayed by an induction time. Such a delay was included in their analysis and its magnitude estimated.

The induction times determined by Dove, Nip, and Teitelbaum are very short, and thus very sensitive to time-origin location. In the H_2 relaxation experiments, the process is very rapid and the calculated $\Delta\rho_o$ is also very sensitive to time-origin location. For the interpretation of such experiments accurate assignment of this point is thus essential. Such an assignment

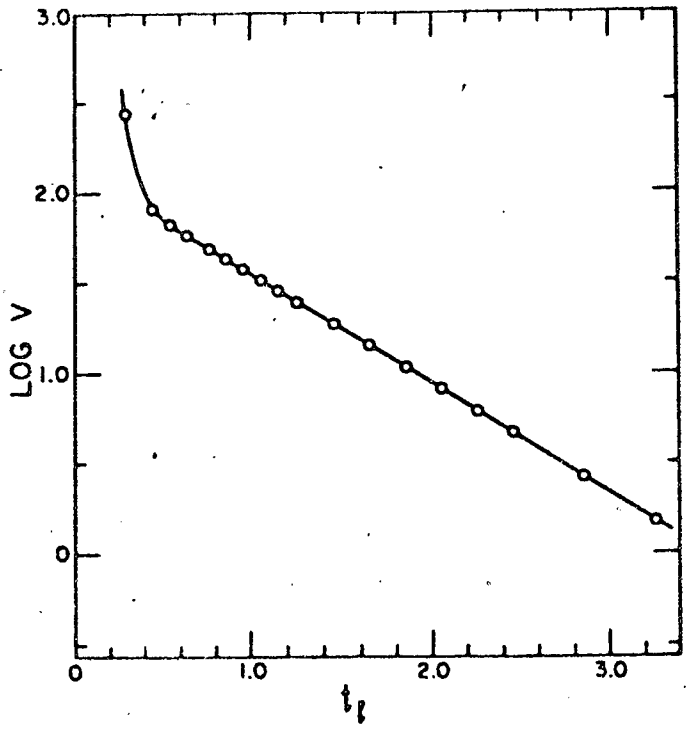

Fig. 4. Plot of logarithm of output voltage (mV) versus laboratory time (μsec) for the oscilloscope trace of Fig. 3. The plot is linear beyond the disturbance due to the shock front. (Courtesy J.E. Dove)

requires, among other things, a realistic treatment of the optics of the beam-shock wave interaction, which we now attempt.

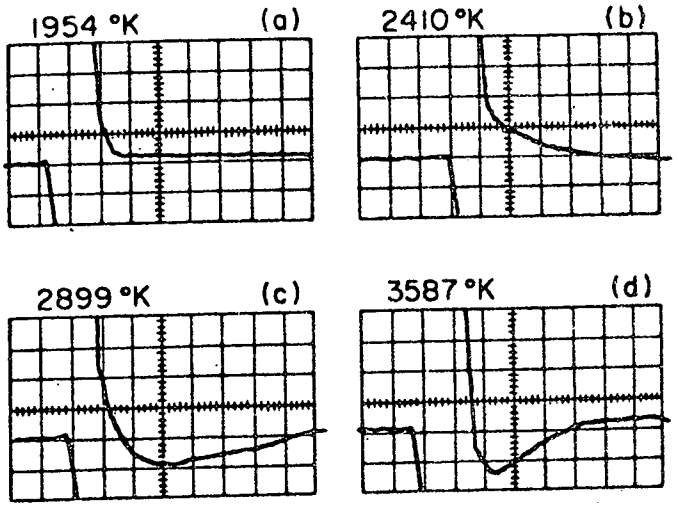

Fig. 5. Examples of schlieren signals from shock waves in 7.97% N_2O in Ar (6). Horizontal scale, 1 major division = 20 mV (corresponds to 2.04% modulation of laser signal). (a) u = 1.435 mm/μsec, P_o = 10.6 Torr, T = 1954 K; (b) u = 1.620 mm/μsec, P_o = 10.1 Torr, T = 2410K; (c) u = 1.796 mm/μsec, P_o = 9.6 Torr, T = 2891 K; (d) u = 2.022 mm/μsec, P_o = 8.5 Torr, T = 3587 K (The origin for all measurements was taken to be the schlieren spike minimum measured from a less amplified trace of the same signal.) (Courtesy J.E. Dove)

III.) PHYSICAL OPTICS OF THE LASER-SHOCK WAVE INTERACTION

Although a real shock wave is three-dimensional, the narrow beam samples a plane section and a two-dimensional treatment is sufficient. Our coordinate system is shown in Fig. 6. Here t = 0 is again the coincidence of shock leading edge and beam center. The distance behind the front is z = x + ut, where x is fixed in the tube as shown and u is the (steady) shock velocity. y is fixed in the detector with origin at detector center and oriented so positive y corresponds to the usual "plus" voltage side of the detector. Then the

differential signal for a rectangular detector of width 2r is

$$\Delta V = V_o \int_{-r}^{r} \mathrm{sgn}(y)\, P(y)\, dy \qquad [4]$$

where V_o is the signal for unit power, and P(y) is the power distribution in the detector plane.

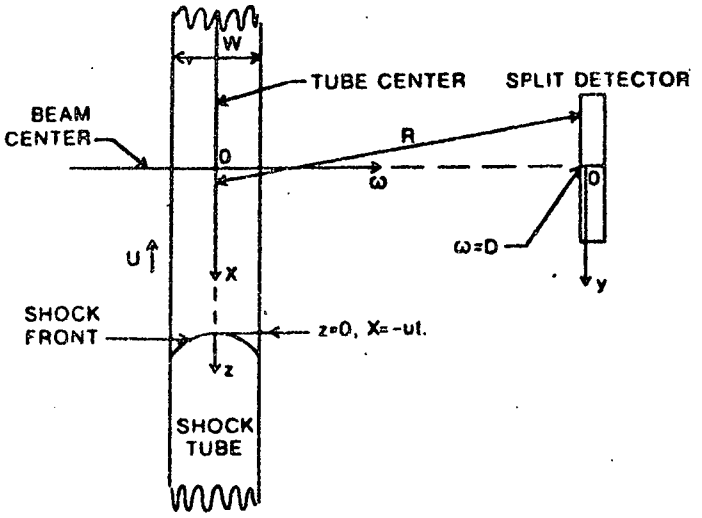

Fig. 6. Coordinate system for the laser beam-shock wave interaction.

The large detector distance effectively collapses the shock tube to a line from which D and R may be measured. That is, any ambiguity introduced by the finite width of the interaction region should be insignificant. We also assume the beam spread and any other distortion arising in passage through the shocked gas are negligible, i.e., the intensity distribution is constant for $|\omega| \leq W/2$. The integrated effect of the gas density on the beam may then be introduced at the source as a "transmission coefficient" T(z). (8).

We may now write the power at the detector in $y \rightarrow y + dy$ as (8)

$$P(y) = A \left| \int_{-\infty}^{\infty} T(z)\, E(x)\, \frac{\exp - (2\pi i R/\lambda)}{R}\, dx \right|^2 \qquad [5]$$

Here E(x) is the field at the shock tube, and A is a constant to be set below. The refractive index field of the shock wave appears in T(z) as

$$T(z) = |T(z)| \exp - \frac{2\pi i}{\lambda} \left[\int_{-W/2}^{W/2} n\, d\omega \right] \qquad [6]$$

Where the real factor $|T(z)|$ is unity for a non-absorbing medium.

For large D we may expand R as

$$R = \left((y-x)^2 + D^2\right)^{1/2} \sim D\left(1 + \frac{(y-x)^2}{2D^2} + O(D^{-4})\right)$$

In the denominator $R \sim D$ is adequate. Cancelling phase factors, inserting $E(x) \alpha \exp - (x^2/a_o^2)$ and normalizing to the total beam power, we have

$$P(y) = P_o\left(\frac{2}{\pi(\lambda D a_o)^2}\right)^{1/2}\left|\int_{-\infty}^{\infty} T(z) \exp - \left[\frac{x^2}{a_o^2} + \frac{\pi i}{\lambda D}(x^2 - 2xy)\right] dx\right|^2 \quad [7]$$

For $T(z) = 1$, we obtain the expected result

$$P(y) = P_o\left(\frac{2}{\pi a^2}\right)^{1/2} \exp - \left(\frac{2y^2}{a^2}\right) \quad [8]$$

with a given by [2].

We begin the application of these equations to a consideration of the response to bulk density variations occuring after front passage, which might model that generated by reactive processes in an ideal shock wave. Here $z >> 0$, $n(z, \omega) = n(z)$ and $|T(z)| = 1$. The power distribution at the detector is given by [6] and [7] as

$$P(y) = P_o\left(\frac{2}{\pi(\lambda D a_o)^2}\right)^{1/2} \int_{-\infty}^{\infty} d\alpha \int_{-\infty}^{\infty} d\beta \exp -(\alpha^2 + \beta^2)/a_o^2$$

$$X \exp - \frac{2\pi i}{\lambda D}\left[WD\left(n(\beta + ut) - n(\alpha + ut)\right) + \beta^2/2 - \beta y - \alpha^2/2 + \alpha y\right]$$

Define new variables through $\beta = \delta + \gamma/2$, $\alpha = \delta - \gamma/2$, and expand as

$$n(\beta + ut) - n(\alpha + ut) = n(\delta + ut + \gamma/2) - n(\delta + ut - \gamma/2)$$

$$= n'(\delta + ut)\gamma + n'''(\delta + ut)\gamma^3/24 + O(n^V\gamma^5)$$

Now $\Theta = Wn'$, so

$$P(y) = P_o\left(\frac{2}{\pi(\lambda D a_o)^2}\right)^{1/2} \int_{-\infty}^{\infty} d\delta \int_{-\infty}^{\infty} d\gamma \exp -(2\delta^2 + \gamma^2/2)/a_o^2 \quad [9]$$

$$X \exp - \frac{2\pi i}{\lambda D}\left[\theta D\gamma + \theta'' D\gamma^3/24 + \ldots + (\delta - y)\gamma\right]$$

If we now assume linear detection, i.e., the magnitude of Θ and its derivatives is small, we may expand as

$$\exp - \frac{2\pi i}{\lambda D}\left[\theta D\gamma + \theta'' D\gamma^3/24 + \ldots\right] \sim 1 - \frac{2\pi i}{\lambda D}\left[\theta D\gamma + \theta'' D\gamma^3/24 + \ldots\right] \qquad [10]$$

For small θ the detector is effectively infinite. Then combining [10] with [9] and [4], and also expanding $\theta(\delta + ut)$, the integration may be done with the result

$$\Delta V = \frac{2\sqrt{2\pi}\, V_o P_o \theta a_o}{\lambda\phi}\left[1 + \frac{\theta'' a_o^2}{6\theta\phi^2} + \ldots\right] \qquad [11]$$

Where $\theta = \theta(ut)$ and $\phi = (1 + (\pi a_o^2/\lambda D)^2)^{1/2}$. This may be compared with the expression of Macdonald, Burns, and Boyd (9)

$$\Delta V = \frac{2\sqrt{2\pi}\, V_o P_o \theta a_o}{\lambda}\left[1 + \frac{\theta'' a_o^2}{8\theta} + \ldots\right] \qquad [12]$$

which may be obtained by setting $\phi = 1$ and neglecting the θ'' term in [10]. The latter constitutes neglect of diffraction by the refractive index field of the shock wave.

Actually the two expressions, [11] and [12], are almost numerically equivalent for the usual parameters, and either may be used to estimate the range over which a direct proportionality of signal and gradient will obtain. Clearly the requirements for this are linear detection, i.e., small deflections, and

$$\frac{\theta'' a_o^2}{8\theta} \ll 1 \qquad [13]$$

To check this inequality, consider an extremely rapid exponential variation $\Theta = \Theta_o \exp -(x + ut)/u\tau$, with $\tau = 0.2\mu$sec (barely resolvable), $u = 2$mm/μsec, and $a_o = 0.3$mm. Then the lhs of [13] is 0.07. The small size of this term for such an extremely rapid process suggests that the proportionality of Θ and ΔV will be quite generally maintained. Equation [11] gives the same correction for $D = 77$cm.

If we neglect diffraction by the refractive index field, i.e., we drop all derivative terms in [9], then the power distribution is

$$P(y) = \frac{2P_o}{\lambda D}\int_{-\infty}^{\infty} \exp - \left(2x^2/a_o^2\right) \exp - \frac{1}{2}\left[\left(\frac{2\pi a_o}{\lambda D}\right)^2 (y - x - \theta D)^2\right] dx \qquad [14]$$

and this is simply a weighted superposition of Gaussians over the detector. The weighting, $\exp - (2x^2/a_o^2)$, is just the incident beam distribution; the detector Gaussians have a radius $\lambda D/\pi a_o$ and are centered at $y = x + \Theta D$. Thus each "ray" of the beam spreads to a radius $\lambda D/\pi a_o$ at the detector. This expanded ray is displaced from detector center by its initial position x and any deflection ΘD. In the absence of deflection, the beam is a parallel bundle of rays, but one in which each ray expands with distance. When D is very large, the usual case, we have ($x = O(a_o)$)

$$\frac{a_o(y - x - \Theta D)}{\lambda D} \rightarrow \frac{\pi a_o}{\lambda}\left(\frac{y}{D} - \Theta\right)$$

and the "memory" of initial ray location is lost.

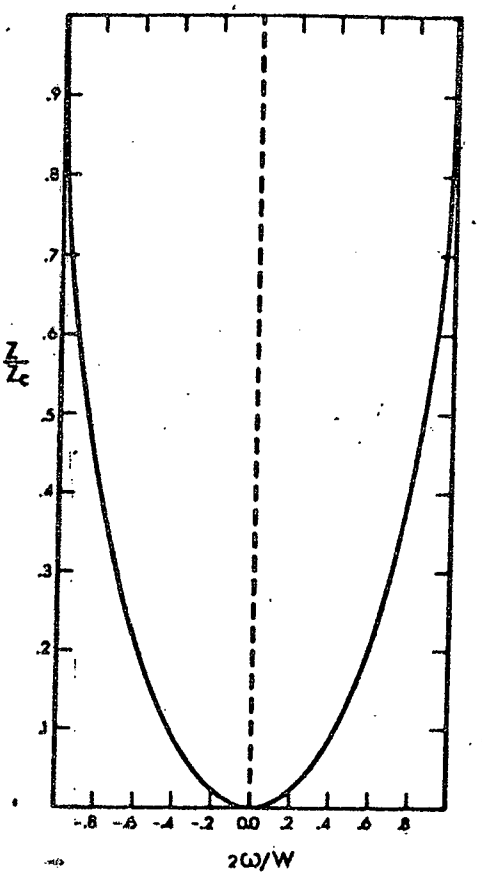

Fig. 7. Shock-front curvature. The line is the theory of de Boer (22) for parallel plane walls. His curve for cylindrical walls is very similar.

To model the signal generated by passage of a curved shock we assume the (rare gas) profile given by de Boer (22) for parallel plane walls, as shown in Fig. 7. We treat the shock as a discontinuity in density and refractive index.

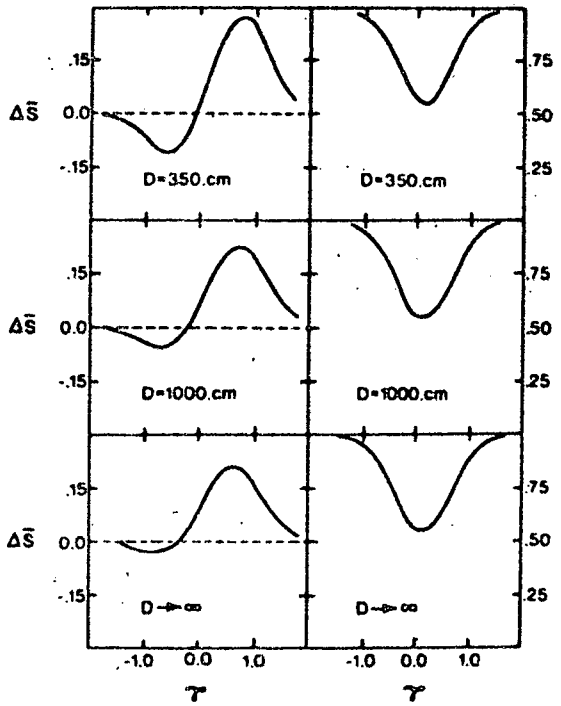

Fig. 8. Calculated schlieren signals for the passage of a curved shock front. The vertical axis is fractional modulation ($\Delta V/V_o P_o$) and the horizontal axis $\tau = ut/a_o$. On the left is the differential response and on the right the summed output of the detector. The shock thickness (axial extent) z_c is 0.39 mm and the detector width 3a, where a is the e^{-2} radius at the detector. Other parameters are as in Fig. 9.

The necessary integrals were evaluated numerically, and the results for a rectangular detector at three distances are displayed in Fig. 8. For comparison the experimental signal generated by an argon shock with parameters similar to those of the D = 350cm simulation is shown in Fig. 9. The shape and magnitude of the simulation and the experiment are quite close, the only evident difference being a slightly larger negative maximum in the simulation.

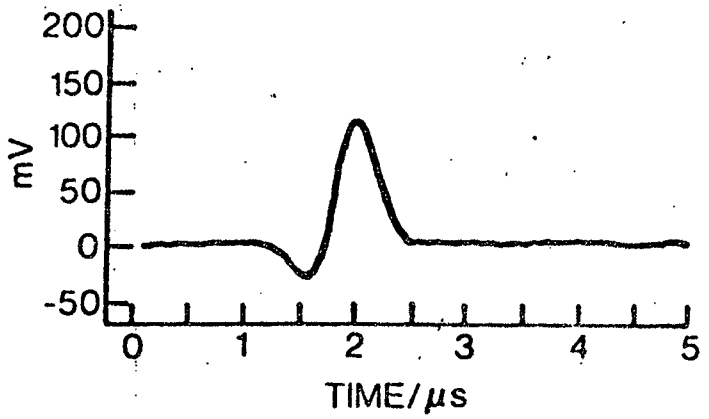

Fig. 9. Laser-schlieren signal generated by a shock in pure argon. The experiment involved detection using a differential photodiode with $u = 1.81$ mm/μsec, $P_o \sim 10$ Torr, $a_o = 0.65$ mm, $D = 350$ and $W = 7.62$ cm. The positive maximum corresponds to a modulation $(\Delta V/V_o P_o)$ of 0.33. (courtesy T. Tanzawa and W.C. Gardiner, Jr.)

Here the ratio of negative to positive maximum is 0.4 whereas it is near 0.25 in the experiment. There could be any number of reasons for this discrepancy - the de Boer curve may be somewhat at fault, the assumed axial extent may be too small, or the negative maximum may be blunted slightly by inadequate response speed in the experiment - and it is impossible to establish a specific cause. Nonetheless the disagreement is minor and should not affect any qualitative conclusions. The time origin - here the coincidence of shock leading edge and beam center - is located on the positive rise near zero-crossing. As the detector distance increases, the negative signal fades and the time origin moves further onto the positive portion. The time from the "first break" in signal to the minimum is $\Delta\tau \sim 1$, or $\Delta t = a_o/u$, which is in agreement with the observations of Tanzawa and Gardiner (20) on argon shocks. Evidently the "first break" is not at radial distance from beam center.

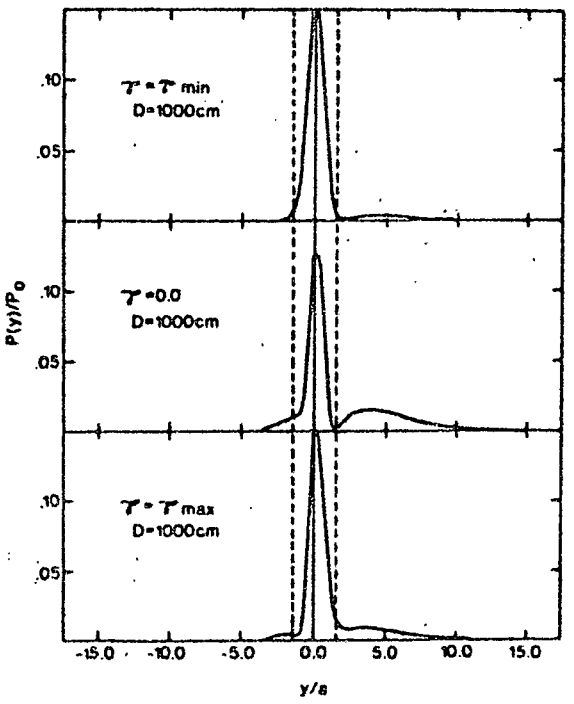

Fig. 10. The power distribution in the detector plane at three characteristic times, the negative maximum, $t = 0$, and the positive maximum. The abscissa is y/a where a is given by equation [2]. The dashed lines indicate the limits of a detector with $r = 1.5a$ (c.f. eq. [4]).

Consideration of the power distribution at various times (c.f. Fig. 10) shows the resulting signal is largely determined by a balance between small deflections from the "tail" of the curve and large deflections resulting in complete removal which are generated by the steep gradients near the leading edge. All deflection is to the positive side of the detector, and neglecting diffraction, a negative signal can only result from preferential removal of radiation initially located on the positive half. However, when the detector distance becomes large, each ray is spread almost equally over both halves and removal produces but small differential result - hence the very small negative signal at large distance (the residual negative signal for $D \to \infty$ arises from diffraction). The small deflections can then dominate even when the leading edge is at beam maximum thereby locating this point on the positive portion of the signal.

If the detector were to be placed very close to the shock tube, the situation would be quite different. There is then a one-to-one correspondence of radiation elements in the incident beam and on the detector. The large deflections which occur as the shock enters the beam now remove energy from the positive side exclusively, producing a large negative signal, and the negative maximum will then very nearly coincide with arrival of the leading edge at beam center. This situation corresponds to the "ray-tracing" model of Dove and Teitelbaum (21) presented at the last symposium. It ignores the diffractive nature of the beam spread and is not valid for the usual large detector distances.

One possible fault of the above analysis is neglect of reflection by the curved front. The reflectivity of the front is difficult to estimate and we have made no attempt to include such reflection. However, since the region likely to reflect strongly, that near the leading edge, produces complete removal through refraction in any case, this neglect is perhaps not serious. Our use of a rectangular detector is motivated by its simplicity. We have also calculated signals for a circular differential detector with results virtually identical to those of Fig. 8.

We now return to the H_2 relaxation (4) (5) and N_2O induction time (6) experiments cited earlier. We have mentioned two effects which can delay the time origin from the negative maximum, which is the origin assumed in both these studies. First there is the small shift from beam diffraction which will

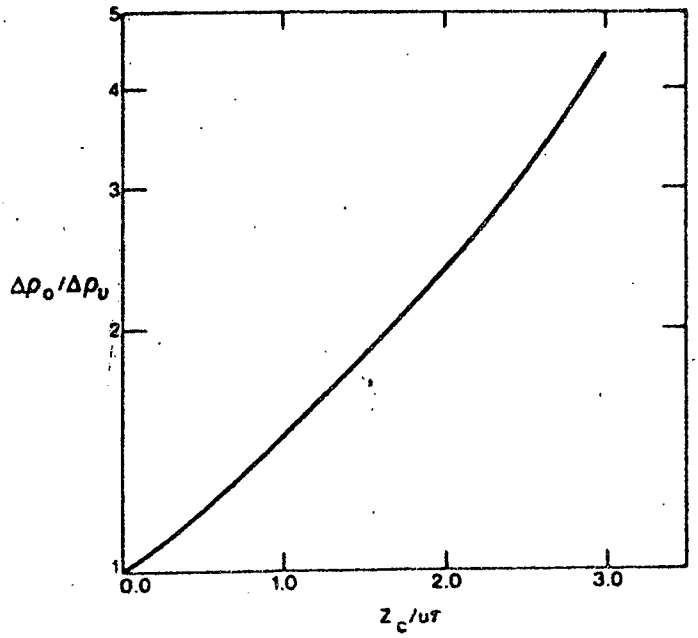

Fig. 11. The effect of shock-curvature averaging on the apparent $\Delta\rho$ for an exponential process. The ordinate is the multiplicative factor [15], the abscissa the ratio of shock axial extent z_c to the characteristic length $u\tau$ of the relaxation.

be 0.2 - 0.4μsec for the experimental conditions used. Second, there is a further delay arising from the axial spread of initiation over the curved shock. We can estimate the latter effect by averaging the amplitude at a later time ($t > z_c/u$), which gives an increase in $\Delta\rho$ by the factor

$$\frac{2}{W}\int_0^{W/2} \exp\,(z/u\tau)\, d\omega \qquad [15]$$

If we assume a parabolic profile, $z = z_c(2\omega/W)^2$, the integral may be easily performed (numerically) with the result shown in Fig. 11. The reason this ratio can be quite large is evidently the heavy weighting given delayed initiation with a rapid exponential decay. To illustrate the effect of the combined corrections we assume a rapid but resolvable relaxation with τ = 0.3μsec, and $u\tau \sim z_c$. Then the combination of delays predicts a $\Delta\rho_0/\Delta\rho_\nu$ of about 3. Although this is but a very crude estimate, it still suggests that a major portion of the experimental $\Delta\rho$ could be spurious. The induction time measurements in N_2O will also be seriously affected by time origin error. They are very short, less than 1 μsec in the laboratory frame, yet may well be too long.

IV.) CONCLUSIONS

The resolution and measurement of extremely rapid processes - processes having characteristic times in the submicrosecond range - is certainly feasible with the schlieren technique. But the interpretation of such experiments is complicated by shock curvature, boundary layer, and the non-geometrical nature of the laser optics. We have presented a rather rigorous formulation of the optical problem, but a more satisfactory treatment of initiation over the curved shock is clearly needed. Work on this problem is continuing and we hope to be able to present a more complete picture in the near future.

REFERENCES

1. J.H. Kiefer and R.W. Lutz, Phys. Fluids 8, 1393 (1965).
2. J.H. Kiefer in Shock Waves in Chemistry, A. Lifshitz Ed. (to be published by Marcel Dekker, N.Y.).
3. J.H. Kiefer and R.W. Lutz, J. Chem. Phys. 44, 668 (1966).
4. J.E. Dove, D.G. Jones, and H. Teitelbaum, 14th Symposium (International) on Combustion (The Combustion Institute, 1973) p. 177.
5. J.E. Dove and H. Teitelbaum, Chem. Phys. 6, 431 (1974).
6. J.E. Dove, W.S. Nip, and H. Teitelbaum, 15th Symposium (International) on Combustion (The Combustion Institute, 1974) p. 903.
7. O. Svelto, Principles of Lasers, (Plenum, N.Y., 1976).
8. M.V. Klein, Optics (Wiley, N.Y., 1970).
9. R.G. Macdonald, G. Burns, and R.K. Boyd, J. Chem. Phys. 66, 3598 (1977).
10. W.D. Breshears, P.F. Bird, and J.H. Kiefer, J. Chem. Phys. 55, 4017 (1971).

11. H. Teitelbaum, 14th Symposium (International) on Combustion (The Combustion Institute, 1973) p. 217.

12. W.D. Breshears and P.F. Bird, J. Chem. Phys. 56, 5347 (1972).

13. W.C. Gardiner, Jr., J.H. Owen, T.C. Clark, J.E. Dove, S.H. Bauer, J.A. Miller, and W.J. McLean, 15th Symposium (International) on Combustion (The Combustion Institute, 1974) p. 857.

14. K. Tabayashi and S.H. Bauer, Comb. Flame 34, 63 (1979).

15. J.H. Kiefer, J. Chem. Phys. 61, 244 (1974).

16. J.H. Kiefer, J. Chem. Phys. 62, 1354 (1975).

17. D.B. Olson, T. Tanzawa, and W.C. Gardiner, Jr., Int. J. Chem. Kin. 11, 23 (1979).

18. J.H. Kiefer and R.W. Lutz, J. Chem. Phys. 45, 3889 (1966).

19. J.E. Dove and H. Teitelbaum, Chem. Phys. (to be published).

20. T. Tanzawa and W.C. Gardiner, Jr., Private Communication.

21. J.E. Dove and H. Teitelbaum, Shock Tube and Shock Wave Research, Proceedings of the 11th Int'l. Symposium on shock tubes and waves, Seattle (1977) p. 474.

22. P.C.T. de Boer, Phys. Fluids 6, 962 (1963).

23. J.H. Kiefer and R.W. Lutz, J. Chem. Phys. 44, 658 (1966).